[Geophysical Research Letters]

Supporting Information for

Seasonal Dependent Impact of Ice-Cloud Longwave Scattering on the Polar Climate

Yi-Hsuan Chen[1*], Xianglei Huang[1], Ping Yang[2], Chia-Pang Kuo[2†], Xiuhong Chen[1]

[1]Department of Climate and Space Sciences and Engineering, the University of Michigan at Ann Arbor, Ann Arbor, Michigan, USA.

[2]Department of Atmospheric Sciences, Texas A&M University, College Station, Texas, USA.

Corresponding author: Yi-Hsuan Chen (yihsuan@umich.edu)

*Current affiliation: Program in Atmospheric and Oceanic Sciences, Princeton University, Princeton, New Jersey, USA.

†Current affiliation: Department of Atmospheric Sciences, Colorado State University, Fort Collins, Colorado, USA

Contents of this file

Introduction

This document includes additional texts, figures, and tables, to add to the argumentation in the main article.

Text S1

Among ~30 global climate models that participated in the IPCC the fifth assessment, only models from three climate modeling centers have taken cloud longwave scattering into account, i.e., CanCM4 and CanESM2 by the Canadian Centre for Climate Modeling and Analysis, HadCM3 by the Hadley Centre, and GISS Model E and E2 by NASA Goddard Institute of Space Science. Further details of their treatments of longwave scattering are summarized in Kuo et al. (2020)

Text S2

We carried out CESM1.1.1 simulations with CAM4 physics (Neale et al., 2010a) in both slab-ocean and prescribed SST simulations (the component was set to "E2000" and "F2000", respectively), but replacing the longwave and shortwave radiation schemes with RRTMG_LW and RRTMG_SW, respectively. RRTMG_LW and RRTMG_SW are the radiation schemes used in CAM5 physics (Neale et al., 2012) and the radiation scheme configuration change can be configured using the scripts in the CESM 1.1.1 package. All simulations are forced with recent forcings at the level of year 2000. Solar forcing is prescribed without year-to-year variation. The horizontal resolution of the simulations is 1.9^{o} latitude by 2.5^{o} longitude and the number of vertical levels in the atmospheric model is 26. Previous study has shown that, compared to satellite observations, the CESM1 can simulate Arctic ice cloud over reasonably well for all seasons (Kay et al., 2016). Similar to many other climate models, the CESM1 tends to have insufficient supercooled liquid water cloud in the polar regions (Morrison et al., 2019).

All experiments are carried out with four ensemble runs. Each run begins with a slightly different initial condition, in which a small, random perturbation is imposed to the initial temperature fields. Technically, we set the CESM1.1.1 namelist variable "pertlim" to 0, 10^{-14}, 2×10^{-14}, and 3×10^{-14} for respective ensemble members. This is similar to the setting used in the CESM Large Ensemble Project (Kay et al., 2015). All members run for 35 simulated years, and the last 30 years are analyzed.

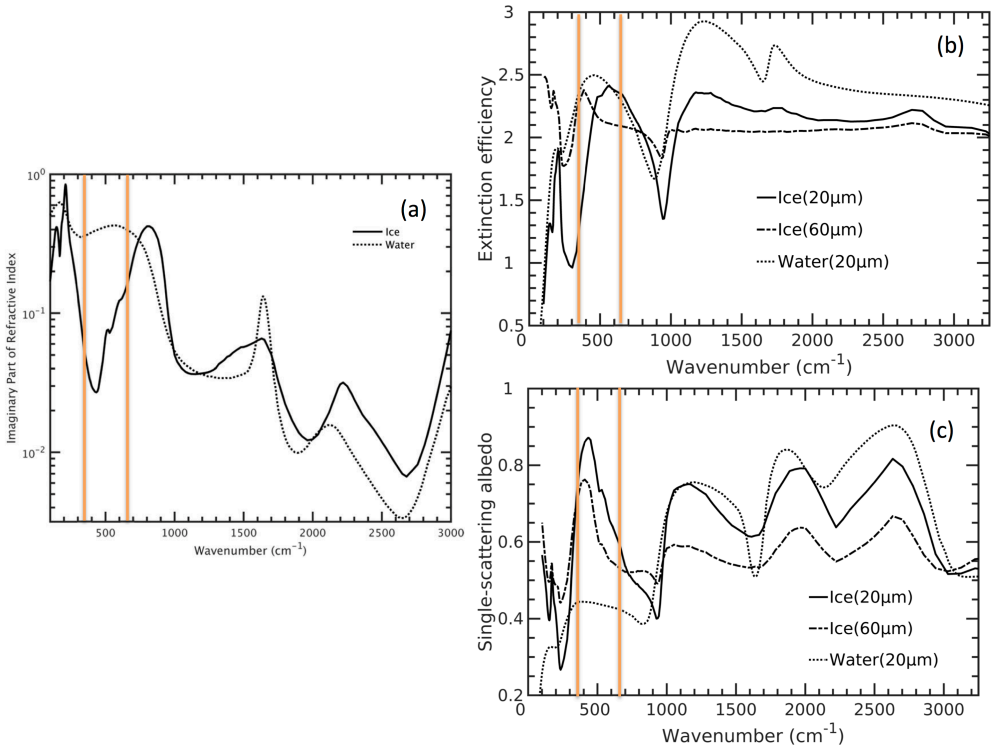

Figure S1: (a) The imaginary part of the index of refraction for ice (solid line) and liquid water (dotted line) in the longwave. (b) The extinction coefficients of ice particles and water droplets as a function of frequency in the longwave. The effective diameters of ice particles are 20 μm (solid line) and 60μm (dashed line), respectively. The effective diameters of water droplets are assumed to be 20 μm. (c) Same as (b) but for the single-scattering albedo. More details about the light scattering calculations for (b) and (c) can be found in Kuo et al. (2017). The two vertical orange lines bracket 350 to 630 cm^{-1}, the bandwidth for two consecutive RRTMG_LW bands in the far-IR.

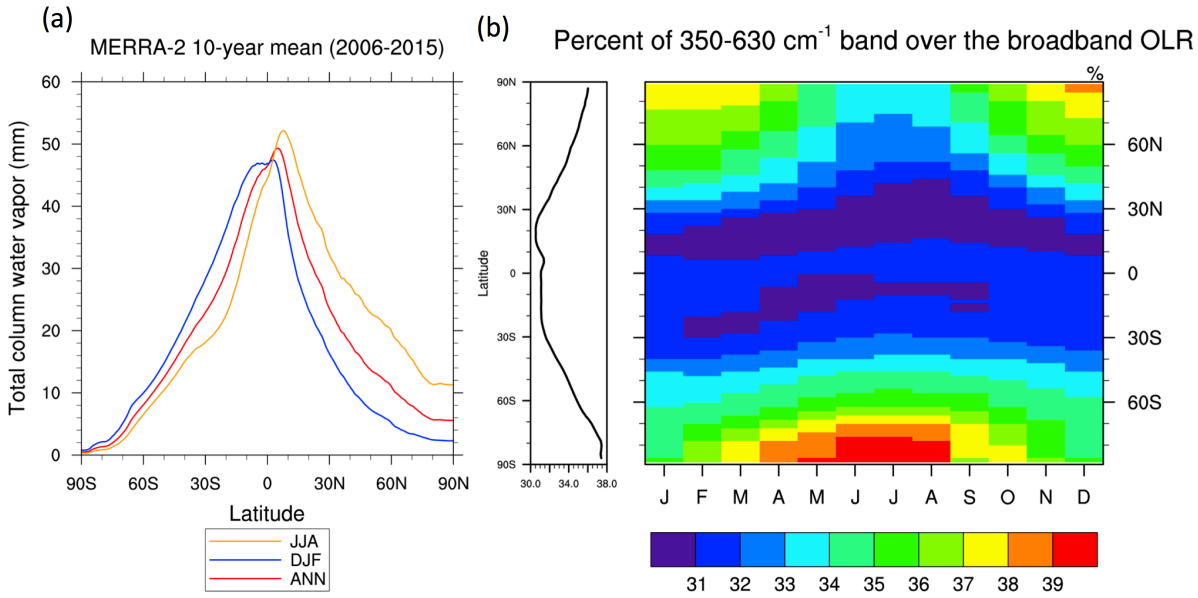

Figure S2. (a) A 10-year (2006-2015) zonal-mean climatology of total column water vapor derived from the NASA MERRA-2 reanalysis. TCWV averages for JJA, DJF, and the annual mean are plotted in orange, blue, and red, respectively. (b). Two plots are both based on spectral flux derived using the method in Huang et al. (2014) from collocated CERES and AIRS observations. Left panel: Annual-mean percentage contribution of 350-630cm^{-1} flux to the entire outgoing longwave radiation (OLR) as a function of latitude in the same 2006-2015 period. Right panel: Percentage contribution of zonal-mean 350-630cm^{-1} flux to OLR in each calendar month derived from the same 10 years of collocated AIRS and CERES observations.

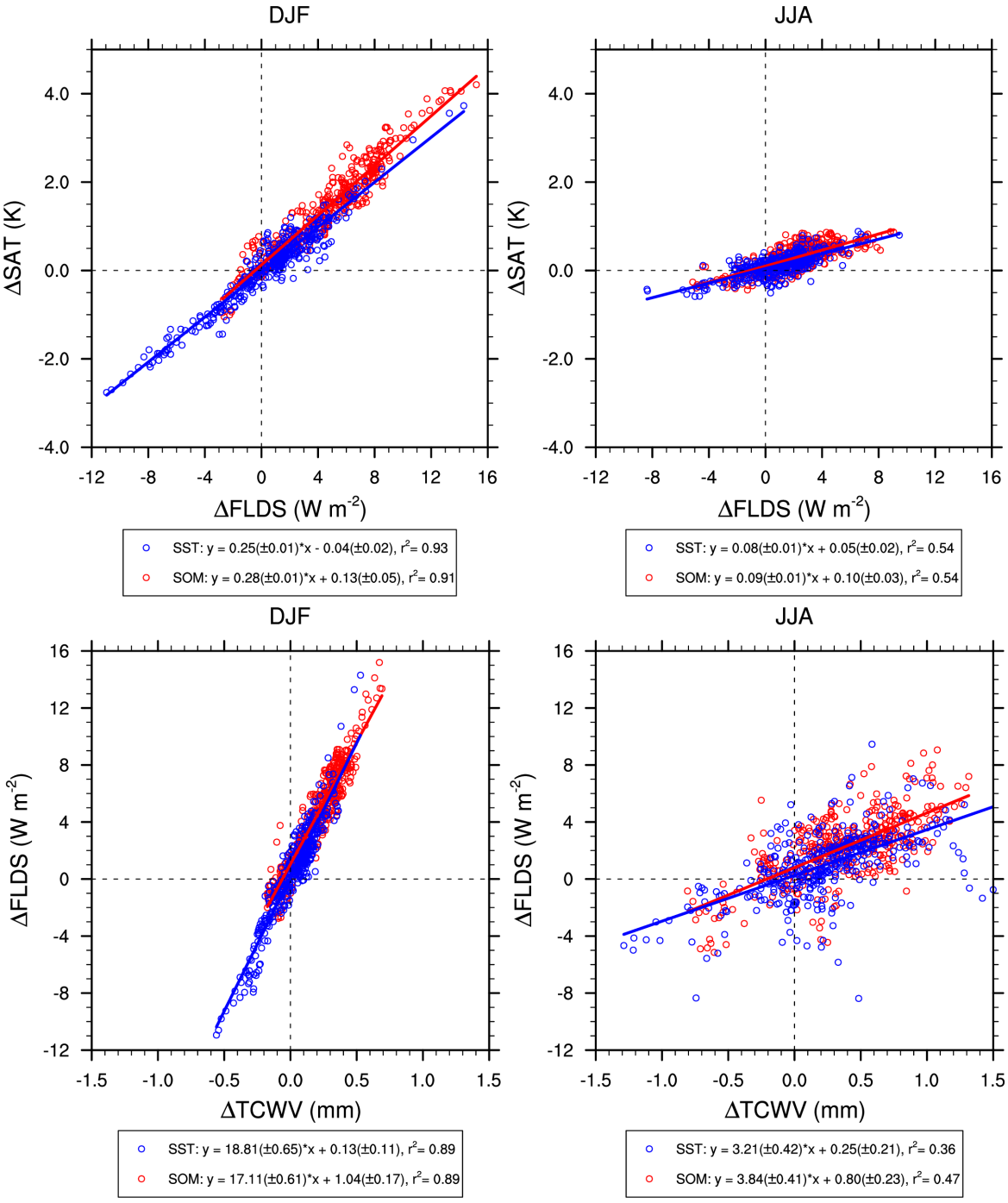

Figure S3. Upper panels: As in Figures 3a and 3d in the text, but using the zonal-mean results instead of Arctic domain-averaged results. The excellent linear relations between ΔSAT and ΔFLDS in DJF hold for the zonal-mean results as well, for both fixed SST and SOM runs. Values of the regressed slopes are also similar to those in Figure 3a. Lower panels: As in Figures 3b and 3e but using zonal-mean results.

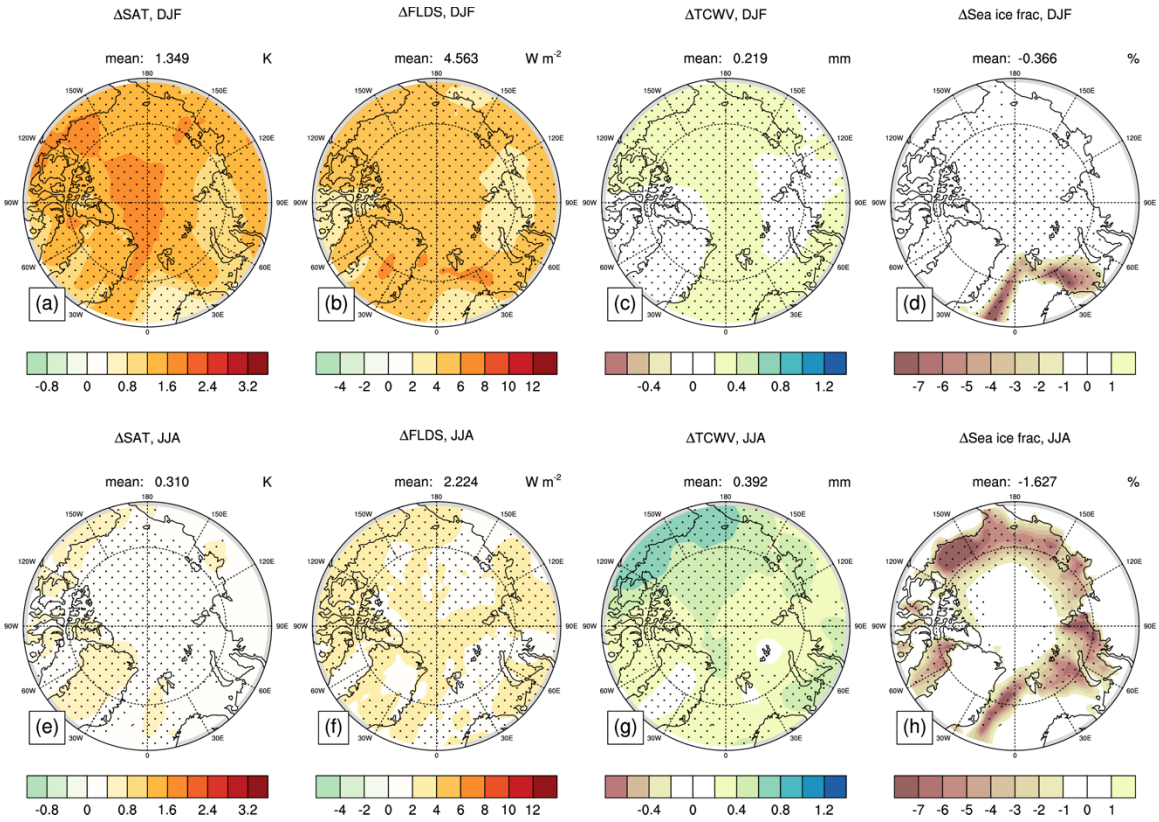

Figure S4. Spatial maps of differences over the Arctic caused by the inclusion of ice cloud scattering (i.e. Scat – noScat) in surface air temperature (SAT), downward longwave flux at the surface (FLDS), total column water vapor (TCWV), and sea ice fraction. The DJF climatological differences are on the top row and the JJA counterparts on the bottom row. The black dots denote grids with statistically significant differences.

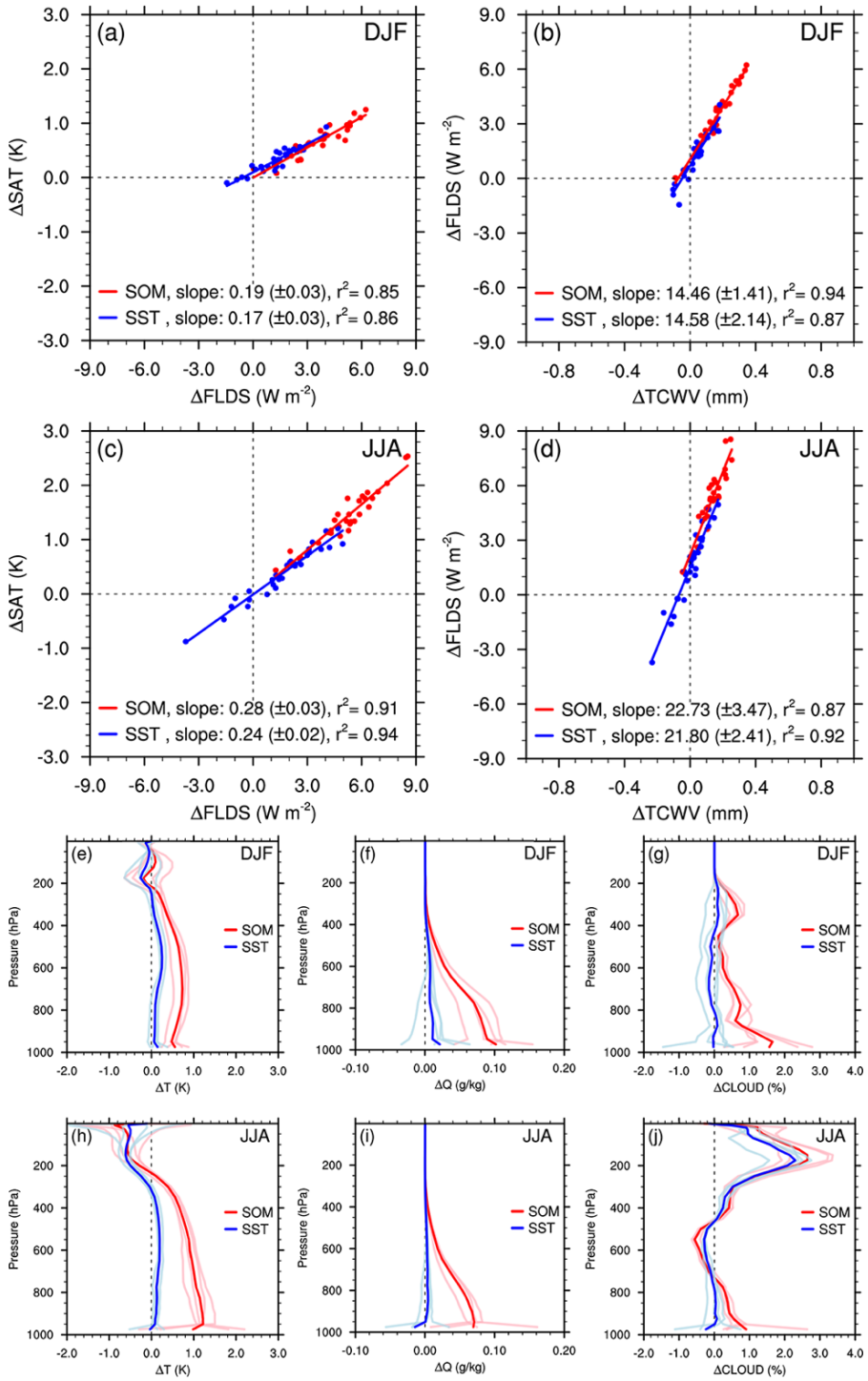

Figure S5. Same as Figure 3 but for the Antarctic.

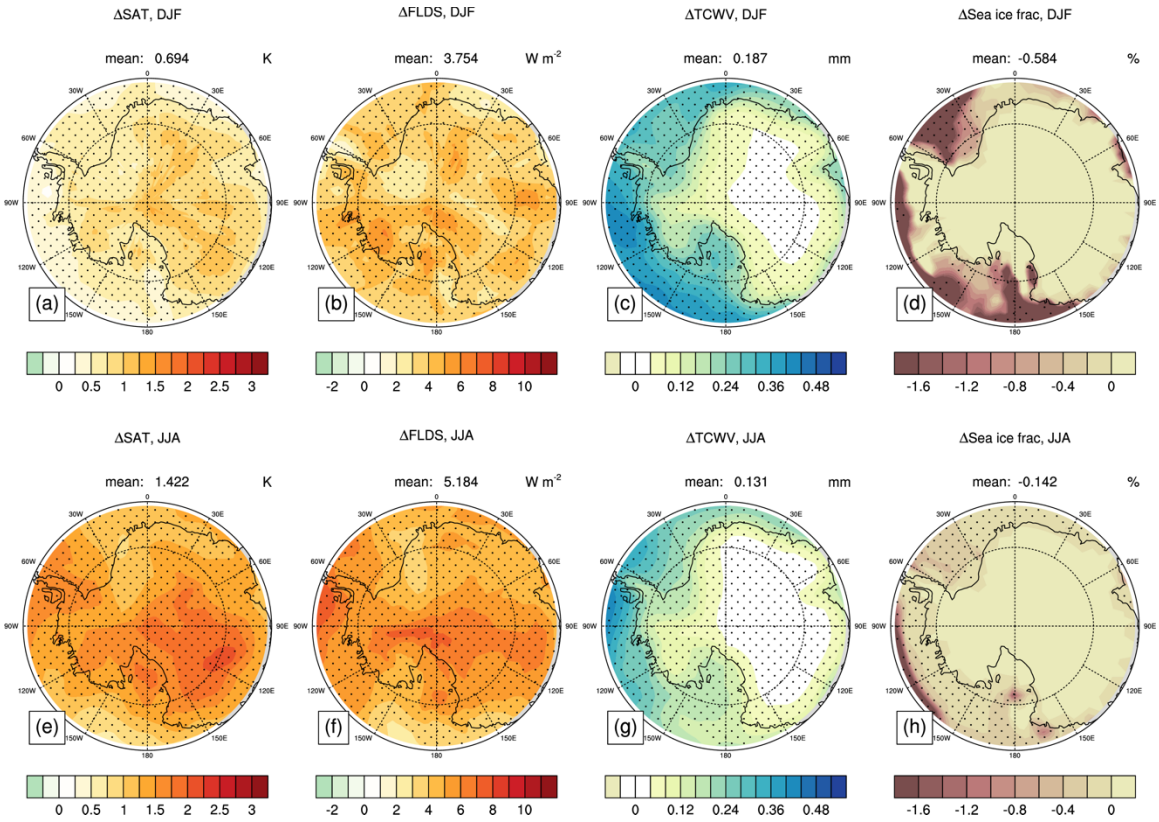

Figure S6. Same as Figure S4 but for the Antarctic.

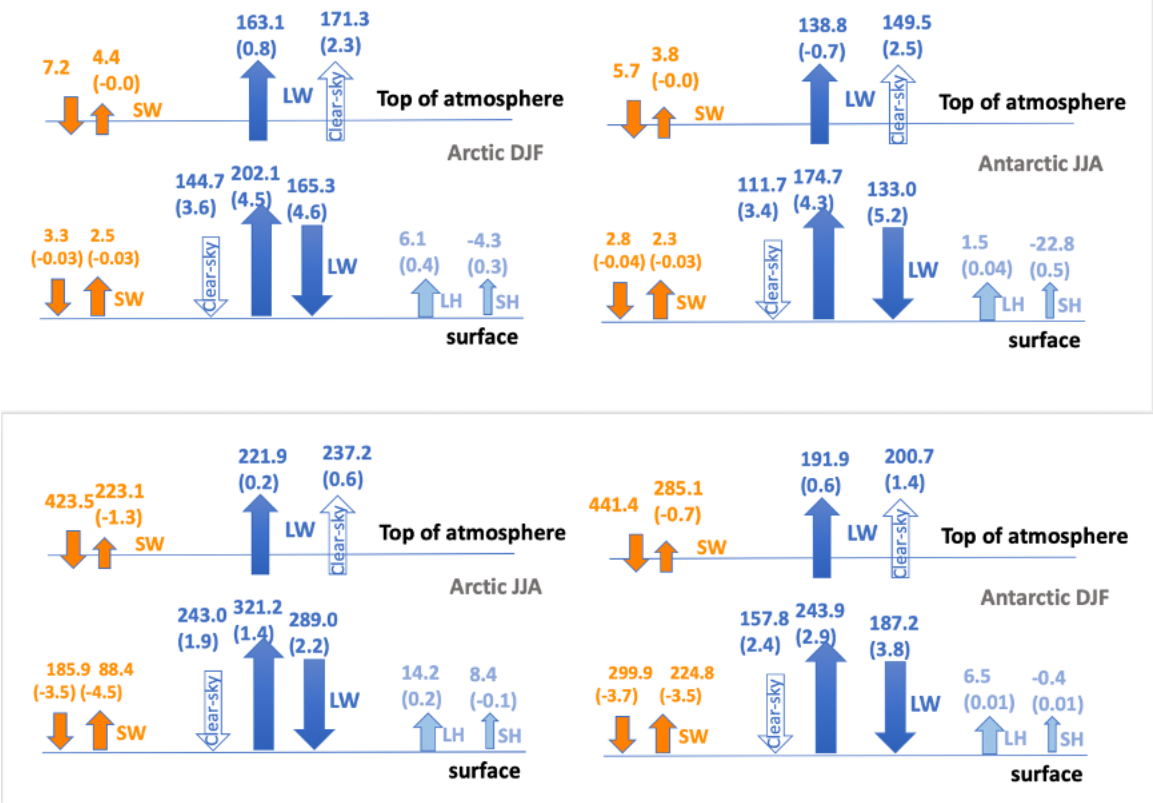

Figure S7. The TOA and surface energy budget for the Arctic and Antarctic. Winter and summer results are shown separately. The numbers outside parentheses are from the ensemble mean of noScat SOM runs. The numbers in the parentheses are the difference between Scat and noScat simulations, i.e., caused by ice-cloud LW scattering. Orange colors are for shortwave components and deep blue for longwave components. The clear-sky LW components are shown as well. The light blue colors are for turbulent heat flux, i.e., latent heat (LH) and sensible heat (SH) fluxes.

Table S1: The linear regression of the Arctic domain-averaged ΔSAT (surface air temperature) with respect to the Arctic domain-averaged ΔFLDS (downward longwave flux at the surface) for each individual ensemble member. The good linear relation in DJF holds consistently for all members.

y:ΔSAT (K) x:ΔFLDS (Wm^{-2})	DJF		JJA	
	Prescribed-SST	SOM	Prescribed-SST	SOM
Member 1	y=0.27(±0.02)x-0.21(±0.12) r^2 = 0.95	y=0.25(±0.03)x-0.12(±0.17) r^2 = 0.93	y=0.10(±0.04)x-0.07(±0.10) r^2 =0.45	y=0.16(±0.05)x-0.08(±0.15) r^2 =0.58
Member 2	y=0.25(±0.02)x-0.08(±0.11) r^2 =0.95	y=0.28(±0.02)x+0.07(±0.15) r^2 =0.96	y=0.10(±0.05)x+0.05(±0.13) r^2 =0.35	y=0.15(±0.04)x-0.05(±0.17) r^2 =0.67
Member 3	y=0.23(±0.02)x+0.00(±0.08) r^2 =0.97	y=0.27(±0.03)x+0.14(±0.17) r^2 =0.94	y=0.07(±0.05)x+0.06(±0.11) r^2 =0.24	y=0.14(±0.04)x+0.01(±0.12) r^2 =0.67
Member 4	y=0.27(±0.04)x+0.02(±0.12) r^2 =0.90	y=0.29(±0.03)x+0.11(±0.19) r^2 =0.94	y=0.08(±0.05)x-0.03(±0.12) r^2 =0.32	y=0.12(±0.04)x+0.14(±0.16) r^2 =0.54

Table S2: The linear regression of the Arctic domain-averaged ΔFLDS (downward longwave flux at the surface) with respect to the Arctic domain-averaged ΔTCWV (total column water vapor) for each individual ensemble member. The good linear relation in DJF holds consistently for all members.

y:ΔFLDS (Wm^{-2}) x:Δ TCWV (mm)	DJF		JJA	
	Prescribed-SST	SOM	Prescribed-SST	SOM
Member 1	y=16.09(±2.07)x+0.26(±0.63) r^2 = 0.90	y=15.71(±1.77)x+1.17(±0.63) r^2 =0.92	y=3.15(±0.94)x+0.15(±0.55) r^2 =0.63	y=3.99(±0.93)x+0.30(±0.57) r^2 =0.73
Member 2	y=15.91(±1.79)x+0.14(±0.54) r^2 =0.92	y=16.56(±1.75)x+0.96(±0.69) r^2 =0.93	y=3.12(±1.36)x+0.23(±0.76) r^2 =0.44	y=3.72(±1.31)x+1.13(±0.98) r^2 =0.55
Member 3	y=14.57(±1.64)x-0.14(±0.54) r^2 =0.92	y=17.32(±1.85)x+0.72(±0.67) r^2 =0.93	y=3.21(±1.03)x+0.02(±0.59) r^2 =0.59	y=4.18(±1.55)x+0.28(±0.94) r^2 =0.52
Member 4	y=14.96(±2.57)x+0.47(±0.57) r^2 =0.84	y=17.32(±1.85)x+0.76(±0.80) r^2 =0.90	y=3.40(±1.19)x+0.65(±0.63) r^2 =0.55	y=3.82(±1.11)x+1.08(±0.82) r^2 =0.64

Table S3: Same as Table 1 but based on Antarctic ensemble-mean results in JJA.

Δ: the difference between Scat and noScat simulations δ: the difference between SOM and SST simulations $\Delta FLDS = \beta_1 \Delta TCWV + c_1$; $\Delta SAT = \beta_2 \Delta FLDS + c_2$; $\Delta SAT = \beta_3 \Delta TCWV + c_3$				
	Prescribed-SST	SOM	δ Difference (SOM - prescribed-SST)	Estimated difference
β_1	**21.8±2.4 (92.5%)**	**22.8±3.5 (86.6%)**		
β_2	**0.23±0.02 (94%)**	**0.28±0.03 (91%)**		
β_3	**4.95±0.98 (79%)**	**5.95±1.56 (69%)**		
ΔT_{700} (K)	**0.20**	**0.90**	**0.70**	
ΔTCWV (mm)	**0.008**	**0.13**	**0.12**	
ΔFLDS (Wm^{-2})	**1.66**	**5.18**	**3.52**	δ(ΔFLDS) = β_1δ (ΔTCWV) **2.6±0.29** **2.7±0.42**
ΔSAT (K)	**0.38**	**1.42**	**1.03**	δ(ΔSAT) = β_1 β_2δ (ΔTCWV) **0.60±0.05** **0.77±0.08** δ(ΔSAT) = β_3δ (ΔTCWV) **0.59±0.12** **0.71±0.19**

Table S4: the surface downward LW flux averaged over the Arctic and Antarctic as simulated by 13 models that participated in the CMIP6 (Coupled model inter-comparison, Phase 6). The AMIP run with prescribed SST is used for this analysis. The CMIP6 model ID and details of each model can be found via https://esgf-node.llnl.gov/projects/cmip6/

CMIP6 models	downward LW flux at surface (Wm^{-2}), 1985-2014			
	Winter Season		Summer Season	
	Arctic DJF	Antarctic JJA	Arctic JJA	Antarctic DJF
BCC-CSM2-MR	196.3	156.9	301.8	209.5
CESM2	194.2	146.0	302.9	201.6
E3SM-1-0	205.9	155.8	309.8	219.3
EC-Earth3	185.1	155.2	291.4	196.1
FGOALS-g3	169.8	133.8	294.1	193.0
GFDL-CM4	182.4	148.9	304.3	206.6
INM-CM5-0	175.8	140.7	292.3	203.8
IPSL-CM6A-LR	184.9	142.3	300.8	199.0
MIROC6	190.8	159.6	308.8	223.6
MPI-ESM1-2-HR	197.3	158.7	304.3	205.9
MRI-ESM2-0	187.0	148.0	304.2	209.5
NESM3	197.5	153.9	301.6	200.4
NorESM2-LM	195.3	144.9	305.6	202.4
standard deviation	9.8	7.9	5.8	8.6